

Superfluidity of Grain Boundaries in Solid ^4He

L. Pollet and M. Troyer

Theoretische Physik, ETH Zürich, 8093 Zürich, Switzerland

M. Boninsegni

*Department of Physics, University of Alberta, Edmonton, Alberta T6G 2J1 and
BEC-INFM, Dipartimento di Fisica, Università degli studi di Trento, Via Sommarive 14, 38050 Povo, Italy*

A.B. Kuklov

Department of Engineering Science and Physics, CUNY, Staten Island, NY 10314

N.V. Prokof'ev and B.V. Svistunov

*Department of Physics, University of Massachusetts, Amherst, MA 01003, USA and
Russian Research Center "Kurchatov Institute", 123182 Moscow, Russia*

By large-scale quantum Monte Carlo simulations we show that grain boundaries in ^4He crystals are generically superfluid at low temperature, with a transition temperature of the order of $\sim 0.5\text{K}$ at the melting pressure; non-superfluid grain boundaries are found only for special orientations of the grains. We also find that close vicinity to the melting line is not a necessary condition for superfluid grain boundaries, and a grain boundary in direct contact with the superfluid liquid at the melting curve is found to be mechanically stable and the grain boundary superfluidity observed by Sasaki *et al.* [Science **313**, 1098 (2006)] is not just a crack filled with superfluid.

PACS numbers: 75.10.Jm, 05.30.Jp, 67.40.Kh, 74.25.Dw

Superfluid grain boundaries (GB) were proposed as a plausible scenario [1–3] to explain the effect of non-classical rotational inertia (NCRI) in solid ^4He discovered by Kim and Chan [4]. An observation by Rittner and Reppy [5] that NCRI signal can be eliminated through annealing was the first explicit evidence that crystalline defects are of crucial importance. The remarkable direct experimental observation of grain boundary superfluidity (at the melting point) by Sasaki *et al.* [6] confirms the early theoretical prediction and marks the beginning of a new stage in the study of the supersolid phase of helium.

In this Letter we expand on our previously reported preliminary results [3] and show that a grain boundary in solid Helium is generically superfluid at low temperatures. The transition temperature, T_c , is strongly dependent on the crystallite orientation: while it is typically of the order of $\sim 0.5\text{K}$, grain boundaries with special relative orientations of the two grains are found to be insulating (non-superfluid). We also obtain strong evidence that a grain boundary in contact with the superfluid liquid, as shown in Fig. 1, is mechanically stable.

This latter question is important for the interpretation of the experimental observation of superflow in crystals with grain boundaries [6]. Since these experiments are carried out under the conditions of phase coexistence between a crystal and a liquid, the observed effect could either be true superflow along a grain boundary, or rather a thin liquid-filled crack in a crystal. The answer depends on the relationship between the three surface tensions, σ_1 , σ_2 , and σ_{gb} (see Fig. 1). Mechanical and energetic

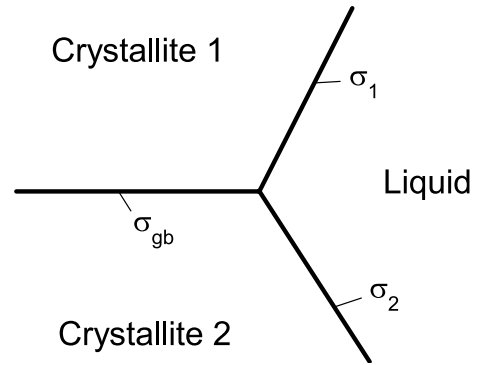


FIG. 1: Sketch of the equilibrium configuration of two crystallites in contact with liquid. The configuration is mechanically stable only if the condition (1) is met. Note that surface tensions σ_1 and σ_2 need not be equal, because of the different orientations of the crystalline axes.

stability of the grain boundary require that

$$\sigma_{\text{gb}} < \sigma_1 + \sigma_2. \quad (1)$$

If this inequality is not satisfied, the liquid penetrates between the two crystallites, and a crack is formed. We will show that this configuration is stable. The grain boundary superfluidity observed by Sasaki *et al.* is thus not merely the manifestation of a crack in the crystal filled with liquid.

Our Path Integral Monte Carlo (PIMC) simulations are based on the continuous-space worm algorithm [7]. For spatial imaging, we employ two slightly different techniques. The first consists of producing *condensate*

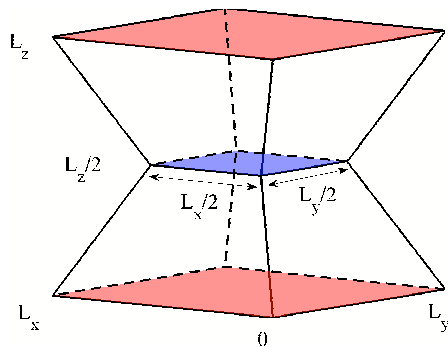


FIG. 2: (Color online) Initial setup for the simulation of a grain boundary in contact with a liquid. Two truncated pyramids are placed on top of each other. The basal plane of both pyramids is a square with size $L_x \times L_y = L \times L$, with $L = 24$ [10]. The upper and lower pyramid have different random orientations and the height of both pyramids is $L_z = L/2$. The upper facets of the truncated pyramids are squares of initial size $L/2 \times L/2$, and form a grain boundary between the two crystallites, indicated by the blue square. Liquid fills the volume outside the crystallites. Periodic boundaries are used in the x and y -directions, while atoms in the $z = 0$ and $z = L$ plane, drawn in red, are pinned, to prevent flow along the boundary in the z -direction. We refer to the Appendix for details such as the exact positions and rotation angles of the crystalline lattices within the pyramids.

maps, which are maps of the condensate wave function, in thin slices of our sample. Within the worm algorithm, this is accomplished by recording spatial positions of the two open ends of the worms, when they are sufficiently far away from each other such that correlations between them are negligible [8]. As a result, the density of points in the map is proportional to the condensate wave function. The second technique is based on the *winding-cycle maps*. Here, we collect statistics of instantaneous particle positions, by considering only particles which participate in macroscopic exchange cycles characterized by non-zero winding numbers, i.e. cycles that directly contribute to the superfluid response [9].

Stability of the grain-boundary–liquid junction. In order to check whether a grain boundary is destroyed when brought into contact with the liquid, we perform a direct simulation of two crystallites in contact with liquid sketched in Fig. 1. Our simulation setup, shown in Fig. 2, consists of two truncated solid pyramids with random crystalline orientation placed on top of each other. The rest of the volume is filled with liquid.

Since the goal of this particular simulation is to study the stability of a grain boundary we can work at a relatively high temperature, $T=0.8$ K, which significantly enhances the performance of the Monte Carlo simulations [11]. The simulation is carried out in the grand canonical ensemble, with the chemical potential fixed at the phase coexistence point. The equilibrium number of atoms in our sample was measured to be about 13660.

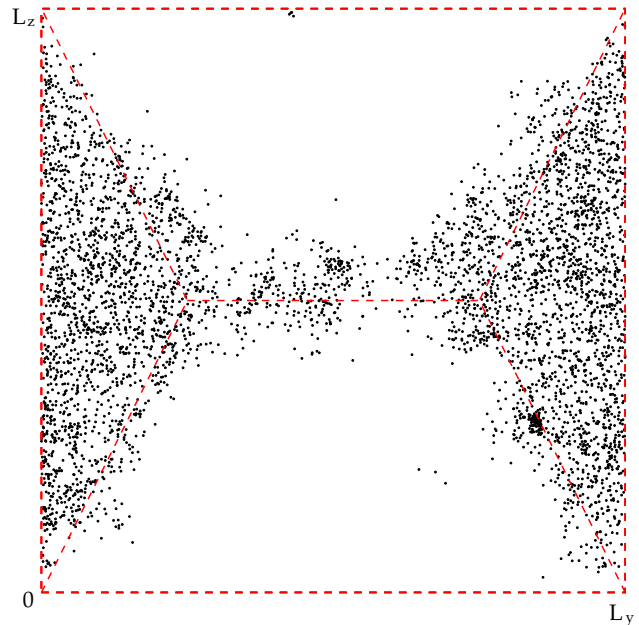


FIG. 3: Condensate map of the two-pyramid sample. The map represents (by the density of points) the condensate wavefunction in the slice $x \in [0.4L, 0.6L]$ averaged over the x -direction. The initial setup is shown by dashed lines.

In order to stabilize the solid phase in the system, we pin (i.e., do not update) solid atoms in the vicinity of the pyramid bases.

In Fig. 3 we show the condensate map of the sample. We see that the grain boundary between the two crystallites is a robust quantum object with a thickness of order 3 (see also Fig. 5) and did not disappear during the simulation run. The system has converged to a state where the liquid and solid phase coexist. Compared to the initial configuration, the shapes of the crystallites (including the angles) have noticeably changed. This is not surprising since the optimal shape of the crystal-liquid interface depends on the particular orientation of the crystallite axes with respect to the interface.

Superfluidity of grain boundaries. Having confirmed the stability and superfluidity of grain boundaries in a generic sample, we next perform a more systematic study of the properties of grain boundaries, extending our previously reported simulations [3], where the superfluidity had been observed, but only for one particular polycrystalline structure, and grain boundary superfluidity could not clearly be distinguished from grain edge superfluidity.

The simulation of a grain boundary between two truncated pyramids with basal length $L = 24$ is computationally very expensive since it requires ~ 13660 atoms, and is by far the largest simulation of solid Helium performed to date. Reducing the size of the pyramids is not an option, since the typical width of the superfluid grain boundary region, estimated from Fig. 3 (see also Fig. 5),

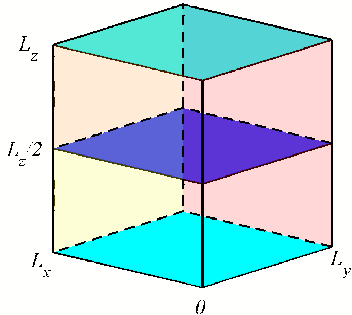


FIG. 4: (Color online) Sketch of the initial of two cuboid crystallites with a total of about 2000 atoms placed on top of each other. The basal plane of both cuboids is a square with size $L_x \times L_y = L \times L$, with $L = 12$. The upper and lower cuboid have different random orientations (see the Appendix for more details). The height of both cuboids is $Lz/2 = 7$, yielding a grain boundary in the $z = 0$ plane (light blue) and a grain boundary in the $z = Lz/2$ plane (dark blue). Periodic boundary conditions are used along all directions, but motion across the xz boundary was suppressed by pinning all atoms at a distance smaller than 0.75 from the $y = 0$ ($y = L_y$) boundary indicated in red. This ensures that any superfluid response in the x -direction is due to the superfluidity of two horizontal grain boundaries[12]. An additional grain boundary due to periodic boundary conditions arises for each crystallite at the $x = 0$ ($x = L_x$) plane (yellow and orange for the lower and the upper cuboid, respectively), but these do not affect the superfluid response in the x -direction.

is ~ 3 . Hence, in the two-pyramid samples of linear sizes significantly smaller than $L = 20 \div 30$, the grain boundary is not well defined, and the system is not supposed to be metastable. For instance, in a sample with $L = 12$, we found that the grain boundary and the two crystallites (apart from the pinned atoms) melt.

To study the properties of generic grain boundaries we use the different sample geometry shown in Fig. 4 consisting of 2000 atoms. Two cuboids of equal size and with random crystalline-lattice orientations are placed on top of each other along the z -direction, which creates two parallel grain boundaries in the xy -plane due to periodic boundary conditions.

An important result of our simulations is that, as already observed in our preliminary studies [3], *not all grain boundaries in the hcp ^4He crystal are superfluid*. Grain boundaries featuring an extra symmetry such as stacking faults and special grain boundaries with nicely matching angles similar to the one shown in Fig. 6, are insulating.

The generic case, however, are superfluid grain boundaries. Results of a typical simulation at $T = 0.25$ K and $n = 0.0287 \text{ \AA}^{-3}$ (melting density) are shown in Fig. 5. The winding-cycle map clearly reveals superfluidity along the x -direction. Based on the relatively large system size

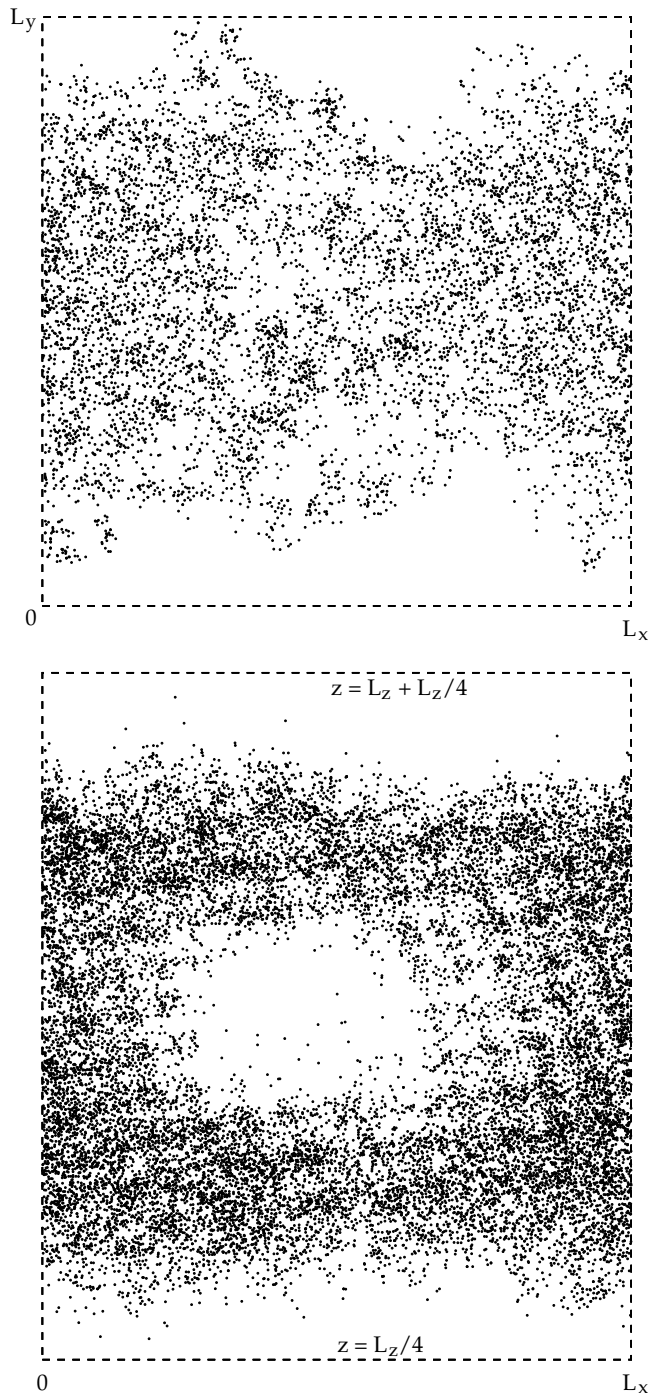


FIG. 5: Phase coherence properties (winding-cycles maps) of grain boundaries in the ^4He sample shown in Fig. 4. Upper panel: projection on the xy plane of the data for the upper half of the sample containing one of the two grain boundaries. Lower panel: (z -shifted) projection of all the data points on the xz plane. Note that the $x = 0$ ($x = L_x$) grain boundary (induced by boundary conditions) of one of the two crystallites turned out to be insulating. This is yet another example of insulating grain boundary with special orientation of crystalline axes.

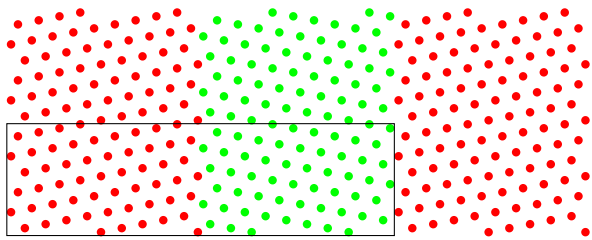


FIG. 6: Example of an insulating grain boundary. This grain boundary is between two crystallites that differ only by a rotation about the axis perpendicular to the base plane. Shown in the figure is a base plane. The rectangular box is the actual simulation cell, the rest being a periodic continuation of the sample. Even with this moderate system size, it is clearly established that the grain boundary is not superfluid. Decreasing the angle between the two crystallites strengthens the insulating character, due to the better match between the atoms of different crystallites. In the small-angle limit, this grain boundary can be viewed as an array of dislocations; the latter are inevitably insulating, given the fact that even at moderate angles the grain boundary is not superfluid.

utilized in this study, we argue that our observed superfluid signal reflects macroscopic grain boundary superfluidity, and is not an artifact, due for example to the vicinity of a superfluid ridge — the intersection of the grain boundary of interest and the additional grain boundary caused by periodic boundary conditions at $x = 0$ ($x = L$). Incidentally, we note that in the area close to the ridge, of size ~ 3 , the density of the map is significantly increased, which is consistent with our general observation that nearly all ridges have robust phase-coherence properties.

An interesting observation is that the density in the vicinity of superfluid grain boundaries is close to that of the crystal, which again confirms that the superflow along the grain boundary is not a liquid-filled crack.

On the basis of a number of simulations similar to the one presented in Fig. 5, performed at different pressures, temperatures, and crystallite axes orientations, we conclude that generic grain boundaries are superfluid with typical (orientation dependent) transition temperatures of about half a Kelvin. The width of the superfluid grain boundary region is ~ 3 . We conjecture that the maximum possible T_c for grain boundary should be at least smaller than the transition temperature of the overpressurized liquid of the same density as the crystal. By simulating superfluid properties of the overpressurized liquid, we found the transition temperature at the density $n = 0.0287 \text{ \AA}^{-3}$ to be $1.5(1) \text{ K}$. We thus take this value as the upper bound for grain-boundary T_c at the melting pressure.

In order to provide a further assessment of the robust-

ness of our conclusions, we have repeated the same study, replacing helium with molecular *para*-hydrogen, at the same low temperatures. In this case, individual particles have a mass which is half that of helium atoms, whereas the interaction potential is approximately three times deeper. No evidence of superfluidity was ever observed in this case, in agreement with experimental findings [13].

Summarizing, based on a direct quantum Monte Carlo simulation of a grain boundary in *hcp* ^4He in contact with liquid under the conditions of phase coexistence, we argue that it is thermodynamically stable against dissolution into two crystallites separated by a crack. This lends theoretical support to the observation of Sasaki *et al.* [6] of generic superfluid grain boundaries. We have studied superfluid properties of grain boundaries and found that special grain boundaries of higher symmetry are insulators. On the other hand, grain boundaries of a general form are found to be superfluid, with typical transition temperatures of the order of $\sim 0.5 \text{ K}$.

While these results lend support to an explanation of the results of Kim and Chan [4] as grain boundary superflow, the direct relevance of these findings to the experiment by Kim and Chan is open, until the presence or absence of grain boundaries is investigated by X-ray or neutron scattering experiments on the torsional oscillator cells used in these experiments.

We thank S. Balibar, M. Chan, R. Hallock, and J. Reppy for fruitful discussions. This work was supported by the Swiss National Science Foundation, as well as the US National Science Foundation under Grants Nos. PHY-0426881, PHY-0426814 and PHY-0456261, and by the Natural Science and Engineering Research Council of Canada, under research grant 121210893. NP gratefully acknowledges hospitality and support from the Pacific Institute of Theoretical Physics, Vancouver (BC). Part of the simulations were performed at the Hreidar cluster at ETH Zurich. LP, BS and MT acknowledge support of the Aspen Center for Physics.

APPENDIX : PREPARATION OF THE INITIAL SAMPLE

Euler angles

The rotation from the x, y, z frame to the $x'y'z'$ -frame is completely determined by the three Euler's angles (θ, ϕ, ψ) . The first rotation is by an angle ϕ about the z -axis, the second is by an angle $\theta \in [0, \pi]$ about the x -axis, and the third by an angle ψ about the z -axis (again). The transformation matrix \mathbf{U} , defined as $\mathbf{r} = \mathbf{r}_0 + \mathbf{U} \mathbf{r}'$, reads:

$$U = \begin{pmatrix} c\psi c\phi - c\theta s\psi s\phi & c\psi s\phi + c\theta s\psi c\phi & s\theta s\psi \\ -s\psi c\phi - c\theta c\psi s\phi & -s\psi s\phi + c\theta c\psi c\phi & s\theta c\psi \\ s\theta s\phi & -s\theta c\phi & c\theta \end{pmatrix} \quad (\text{A.2})$$

where c is a shorthand notation for \cos and s for \sin .

Construction of the initial sample with the pyramids, see Fig. 2

Based on the crystallographic definition of the $x'y'z'$ -system, the position of the first atom, $\mathbf{r}' = (0, 0, 0)$, unambiguously defines an infinite *hcp* lattice, of which we take only the atoms whose positions are inside the pyramid. The randomly selected values which specify the initial configuration of the lower crystallite are shown in Table I.

parameter	value
x_0	34.946
y_0	24.507
z_0	0.87081
θ	1.9978
ϕ	4.0671
ψ	2.3174

TABLE I: Initial parameters for the lower pyramid.

The second pyramid is constructed similarly, and then mirrored with respect to the $z = L/2$ plane. The randomly selected values which specify the initial configuration of the upper crystallite are shown in Table II.

parameter	value
x_0	3.9613
y_0	37.245
z_0	19.288
θ	0.98923
ϕ	1.0833
ψ	1.9885

TABLE II: Initial parameters for the upper pyramid.

The initial positions of atoms of the liquid component are selected at random. The liquid fills the volume outside the crystallites.

Construction of the initial sample with the cuboids, see Fig. 4

The initial sample has about 2000 atoms consisting of two cuboid crystallites placed on top of each other along the z -direction. The crystallites were prepared in the same way as the pyramids in Section : we choose a random position \mathbf{r}_0 and random Euler angles (θ, ϕ, ψ) in order to specify the offset and the orientation of the crystallites versus the simulation box. There is no liquid phase in the initial sample. The values of the initial parameters of the lower cuboid are shown in Table III.

The values of the initial parameters of the upper cuboid are shown in Table IV.

parameter	value
x_0	34.946
y_0	24.507
z_0	1.0160
θ	1.9978
ϕ	4.0671
ψ	2.3174

TABLE III: Initial parameters for the lower cuboid.

parameter	value
x_0	6.6684
y_0	28.603
z_0	19.706
θ	2.1532
ϕ	4.7702
ψ	6.0979

TABLE IV: Initial parameters for the upper cuboid.

-
- [1] N. Prokof'ev and B. Svistunov, Phys. Rev. Lett. **94**, 155302 (2005).
 - [2] E. Burovski, E. Kozik, A. Kuklov, N. Prokofev, and B. Svistunov Phys. Rev. Lett. **94**, 165301 (2005).
 - [3] Our preliminary results on superfluidity of grain boundaries in ^4He were reported at the KITP Miniprogram: The Supersolid State of Matter, 6-17 February 2006, http://online.kitp.ucsb.edu/online/smatter_m06/svistunov.
 - [4] E. Kim and M.H.W. Chan, Nature, **427**, 225 (2004); Science **305**, 1941 (2004).
 - [5] A.S.C. Rittner and J.D. Reppy, Phys. Rev. Lett. **97**, 165301 (2006).
 - [6] S. Sasaki, R. Ishiguro, F. Caupin, H.J. Maris, and S. Balibar, Science **313**, 1098 (2006).
 - [7] M. Boninsegni, N. Prokof'ev, and B. Svistunov, Phys. Rev. Lett. **96**, 070601 (2006); Phys. Rev. E **74**, 036701 (2006).
 - [8] M. Boninsegni, N.V. Prokof'ev and B. V. Svistunov, Phys. Rev. Lett. **96**, 105301 (2006).
 - [9] E.L. Pollock and D.M. Ceperley, Phys. Rev. B **36**, 8343 (1987).
 - [10] All distances are measured in units of the mean interparticle distance in the solid phase, $n^{-1/3}$, at the $T=0$ melting density of a ^4He *hcp* crystal, $n = 0.0287\text{\AA}^{-3}$.
 - [11] In real-time dynamics the mobility of the interface is however slower, see S. Balibar, H. Alles, and A. Y. Parshin, Rev Mod Phys **77**, 317, (2005).
 - [12] Otherwise, we would have to deal with the "shunting" superfluid response of grain boundaries arising, by periodicity, within the same crystallite at $y = 0$ ($y = L_y$) interfaces.
 - [13] A. C. Clark, X. Lin, and M. H. W. Chan, condmat/0610240 (2006).